ISSN- 2394-5125 VOL 07, ISSUE 10, 2020

Ni(II) and Hg(II) complexes of 1-formyl-3-semicabazide: DFT, Equilibrium, DNA Binding and Antimicrobial studies.

Anjum Fatima[a] and B.Sireesha[a]*

[a]Deparment of Chemistry, University College of Science, OU., Hyderabad, TS, India
*berleysiree@gmail.com

ABSTRACT

The biologically active semicarbazide derivative1-formyl-3-semicarbazide and its metal complexes with Ni(II) and Hg(II) ion have been synthesized and characterized using LC-MS, IR, UV, NMR,TGA, magnetic susceptibility and conductance. Computational calculations have been carried using DFT RB3LYP method and 6-311(d,p) basis set by GAUSSIAN 16W program. Different parameters were calculated for six possible keto-enol tautomeric forms of FSC. Equilibrium studies of FSC with Ni(II) ion were carried out using Irving Rossetti titration technique. The dissociation constant reveal it to be a monobasic acid while the formation constant suggest 1:1 Ni(II)-FSC complex formation in the solution. DNA Binding studies were carried using absorption, fluorescence emission and viscositymeasurements, revealing intercalation mode of binding of Ni(II)-FSC complex with DNA. The antimicrobial activity carried outusing agar-disc diffusion method revealed that ligand FSC possess good activity than Ni(II), Hg(II)-FSC complexes against gram negative bacteria (E.coli).

Keywords: 1-formyl-3-semicarbazide, DFT, Dissociation constant, Formation constant, DNA Binding studies, Antimicrobial activity.

1. Introduction:

Semicarbazide derivatives exhibit wide spectrum of pharmacological activity. They have also been used as antimicrobial and antiviral agents[1]. The considerable research in the areaof physiological activity of these compounds may be due to their ability to chelate with the metal ions even at low concentrations. Computational studies[2]were used in finding certain parameters which are experimentally difficult to find out. E_{HOMO} and E_{LUMO} aid in calculating the quantum chemical descriptors for knowing the reactivity of the compounds. Equilibrium studies[3]have been used in finding the ligational aspects of the molecule in solution, by calculating the dissociation constants of the ligand and formation constants of the metal complex.The DNA binding studies of the metal complexes have been focused on small molecules in the recent times.The metal complex binding with DNA may be through intercalative modeor groove binding based on the interaction of molecules with DNA[4]. In the present study smaller semicarbazide derivative 1-formyl-3-semicarbazide (FSC) and its Ni(II) and Hg(II) complexes were synthesized and characterized. Computational and equilibrium studies of FSC; DNA binding studies and antimicrobial activity[5] for its metal complexes have been studied.

2. Experimental

2.1. Materials and methods: The reagents and solvents used were of AnalaR grade. For determining the melting point of the synthesized compounds, Melting point apparatus of make Remi has been used. The purity of the compound was confirmed by using TLC technique. The pH measurements were made using an Elico Electronic model LI-120 pH meter in conjunction with a combined Glass electrode.The IR spectra was recorded on Schimadzu IR prestige-21

ISSN- 2394-5125 VOL 07, ISSUE 10, 2020

FTIR spectrophotometer in the range of 4000-250cm^{-1} using KBr pellets. The ^{1}H-NMR,D_2O exchangeable proton spectra and ^{13}C-NMR, were recorded on Bruker-UXNMR spectrometer using DMSO-d6 solvent and the chemical shifts were reported in ppm using TMS as an internal standard. The mass spectral data were recorded on Shimadzu LCMS-2010A using electron spray ionization technique. The electronic spectra were recorded onSchimadzu UV-3600 series spectrophotometer. Computational studies **has** been carried out using GAUSSIAN 16W program.Molar conductance was measured at room temperature using digital conductivity meter model Global DCM 900. The TGA was recorded in nitrogen atmosphere (20mL.min^{-1}) with heating rate of 10 ^{o}C per minute using Schimadzu TGA-50H thermal analyzer.ESR spectra has been recorded in JES-FA series maintaining the frequency between 9000-9500MHz. The UV-VIS spectra and DNA Binding Absorption studies were recorded on Schimadzu UV-3600 series spectrophotometer. DNA Binding flourescence studies were recorded on Schimadzu spectrofluorometer RF-5301.Viscosity measurements were carried out using Ostwald viscometer. For antimicrobial activity, agar disc diffusion method has been used with gentamicin as an internal standard.

2.2. Synthesis of 1-formyl-3-semicarbazide (FSC): 1-formyl-3-semicarbazide (scheme 1) was prepared by refluxing 3gm (2.68mmol) of semicarbazide with 1.0147mL (2.68mmol) of formic acid[6] for 2hr on water bath. The progress of the reaction and purity of the compound was monitored by TLC. Off-white compound obtained was recrystallized using ethanol:water mixture (3:1).

2.2.1. 1-formyl-3-semicarbazide (FSC) ($C_2H_5N_3O_2$): Yield: 89%. Anal. Calc (%): C, 23.30; H, 4.87; N, 40.76. Found: C, 23.30; H, 4.85; N, 40.77. IR (KBr) (cm^{-1}): ($\upsilon_{N(4)-H2}$) 3186, 3155; ($\upsilon_{N(1)-H}$ amide) 3091; ($\upsilon_{N(2)-H}$) amide) 3020;(υ_{C-H} ald) 2841, 2769;(υ_{CONH2})1701; (υ_{CO}-formyl) 1695 and (υ_{N-N}) 1010.UV-VIS; (λ_{max}/nm (cm^{-1}): 220.500 (45351), 215.500 (46403).^{1}H NMR (400MHz, DMSO-d_6) (δ):11.50(s, 1H, OH), 11.39(m, 1H, OH),8.17 (s, 1H, ald), 7.78(s, 1H, N(1)H), 7.40 (s, 1H, N(2)H) 3.84(m, 2H, NH_2).^{13}C NMR (400MHz, DMSO-d_6) (δ): 155-156 (C=O); 136.09 (C-OH).ESI-MS (m/z):103 [$C_2H_5N_3O_2$], 156[$C_2H_5N_3O_2$+ Na + MeOH]$^{+}$, 124[$C_2H_5N_3O_2$+Na]$^{+}$, 74[CH_4N_3O]$^{+}$, 69[$C_2H_3N_3$]$^{+}$. M.P: 182-185˚C.

2.3. Computational studies: The 1-formyl-3semicarbazide structures was built six tautomeric forms i.e., keto-enol and thione-thiol forms and geometry optimization have been performed using using Hatree-Fock calculation DFT RB3LYP method[7] and 6-311 G (d.p) basis set[8]. The themochemical properties, dipole moment, mulliken charges, bond parameters, HOMO-LUMO surfaces $E_{HOMO,}$ E_{LUMO}[9] and molecular electrostatic mapping has been generated and quantum chemical descriptors have been calculated by following expressions[10-12].

Ionization potential (I) = $-E_{HOMO}$ …….(1)
Electron affinity (A) = $-E_{LUMO}$ ……..(2)
Chemical potential (μ) = $-\chi = -(I+A)/2$ …….(3)
Global hardness (η) = (I-A)/2 ……..(4)
Global softness (S) = 1/η .....(5)
Electro negativity (χ) = (I+A)/2 ……..(6)
Electrophilicity (ω) = $\mu^2/2\eta$ ...…..(7)

ISSN- 2394-5125 VOL 07, ISSUE 10, 2020

2.4. Equilibrium studies: AnalaR grade Ni(II) nitrate have been used to prepare Ni(II) ion solution and standardize with known methods[13]. Irving Rossotti pH titration method[14]have been used in determining pKa of FTSC and formation constants Ni(II)-FSC system in solution. The technique involvesthe titration of: **(1)** HNO_3 (0.004 M) **(2)** HNO_3 (0.004 M) + FSC (0.001 M) **(3)** HNO_3 (0.004 M) + FSC (0.001 M) + Ni^{2+} ion (0.0002 M) in 70% v/v DMF-Water medium and 0.1M (KNO_3) ionic strengthagainst standard 0.1M sodium hydroxide solution. The titrations of FSC were carried out in 70% v/v DMF-water at 303 K temperature and 0.1M (KNO_3) ionic strength with Ni(II) ion and the titration curves have been plotted.Linear plots were plotted to get accurate pKa and stability constant values.The $\bar{n}_A$ and $\bar{n}$ values were calculated using the formulas:

$\bar{n}_A$ = **Total concentration of proton bound to ligand**
Total concentration of ligand not bound to metal ion

$\bar{n}$ = **Total concentration of ligand not bound to metal ion**
Total concentration of metal ion

$$\bar{n}_A = \left[YT_L^0 + \left\{ \frac{(V_1 - V_2)(N + E^0)}{(V_0 + V_1)} \right\} \right] \Big/ T_L^0 \qquad \text{----------} \quad (1)$$

$$\bar{n} = \frac{(V_3 - V_2)[N + E^0 + T_L^0(Y - \bar{n}_A)]}{(V_0 - V_2)\,\bar{n}_A\,T_M^0} \qquad \text{----------} \quad (2)$$

$$pL = \log \frac{\sum_{j=0}^{j=j} \beta_J^H \left(\frac{1}{\text{antilog pH}} \right)^J}{\left(T_L^0 - \bar{n} T_M^0 \right)} * \frac{V_0 + V_3}{V_0} \qquad \text{----------} \quad (3)$$

Where

Y = No. of dissociable protons present in the ligand

T_L^0 = Total ligand concentration

T_M^0 = Metal ion concentration

N = Concentration of base

V_0 = Total initial volume

V_1, V_2, V_3 = Volumes of alkali consumed to reach a given pH value on the titrationcurve of acid, ligand and metal respectively.

β_J^H = Successive overall proton-ligand formation constant.

2.5. Synthesis of metal complexes: M(II)-FSC complexes have been synthesized using metal chloride salts of Ni(II) and Hg(II) ions. Hot ethanolic solution of FSC were mixed slowly with respective metal ion solutionin 1:2 (M:L) ratio with constant stirring. The mixture was refluxed for 6 hrs and the pH of complexation was adjusted by few drops of methanolic ammonium hydroxide solution, further they have been refluxed for two more hours. Off white solid

ISSN- 2394-5125 VOL 07, ISSUE 10, 2020

complexes were separated out, filtered and washed with hot methanol, distilled water, finally with petroleum etherand dried in vacuum.

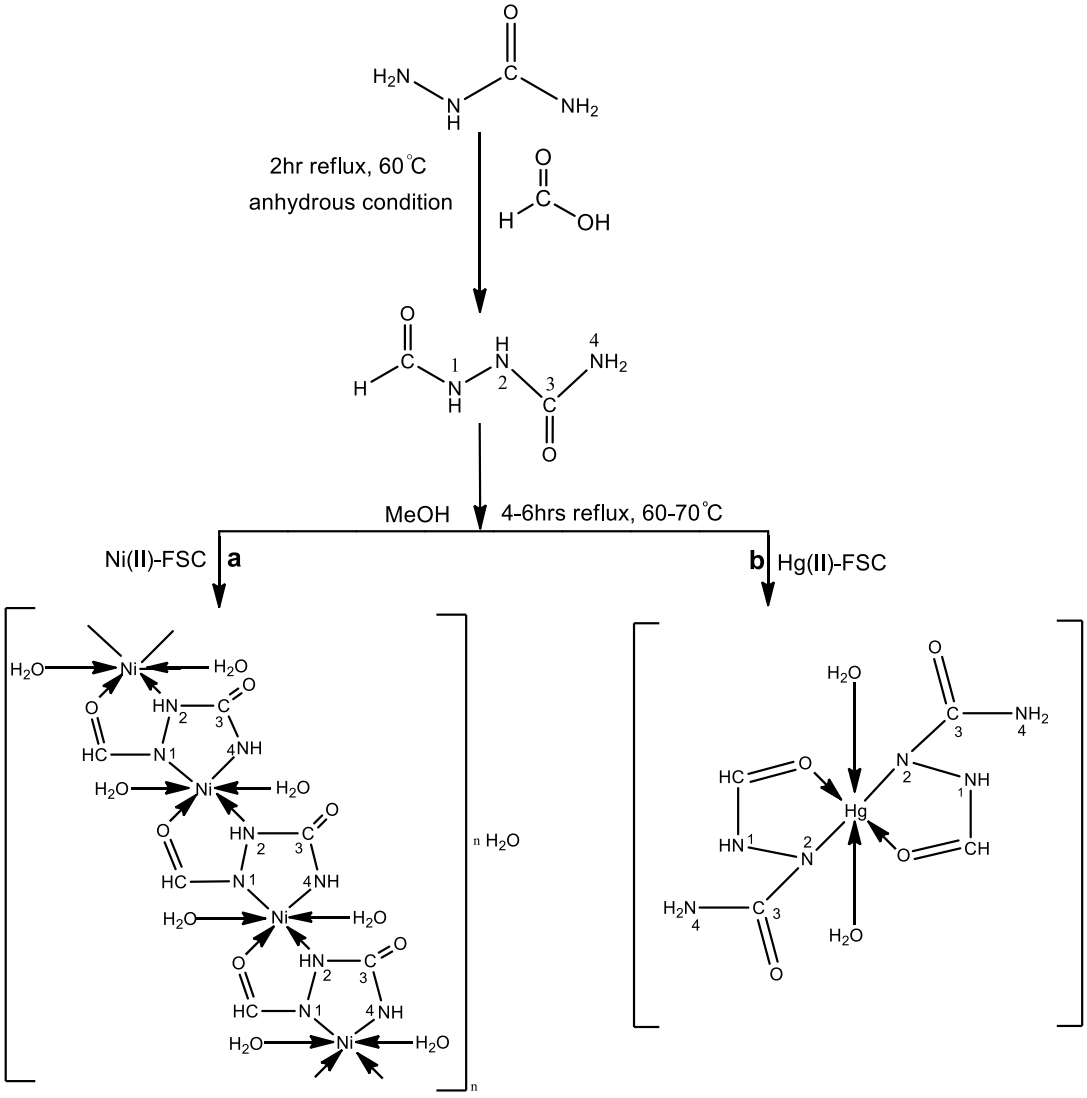

Scheme: Synthesis of FSC and its M(II) complexes

2.5.1. $[NiL(H_2O)_2]_n.nH_2O$ ($C_2H_9NiN_3O_5$) (a): Yield:75%Anal.Calc(%): C, 13.49; H, 2.83; N, 23.61. Found: C, 13.48; H, 2.80; N, 23.59. IR (KBr)(cm^{-1}): ($\upsilon_{N(4)H2}$), 3280; ($\upsilon_{N(2)-H}$),3020; ($\upsilon_{C=O}$),1625. ESR: $g_{\parallel}$=2.1318, $g_{\perp}$=2.0304, G=4.6070 .LC-MS (ESI) (m/z): 196 $[ML.H_2O]^+.H_2O$, 178 $[ML.H_2O]^+$, 159 $[ML]^+$, 58 $[M]^+$.

2.5.2. $[HgL_2(H_2O)_2]$ ($C_4H_{12}HgN_6O_6$) (b):Yield: 79% Anal.Calc(%): C, 10.90; H, 2.74; N, 19.07. Found: C, 10.90; H, 2.74; N, 19.09. IR (KBr) (cm^{-1}): ($\upsilon_{N(1)H}$), 3138; ($\upsilon_{C=O}$), 1606.^{1}H-NMR (400MHz, DMSO-d_6) (δ, ppm): 13.6 (s, N(2)H); 8.2-7.9, (2H, NH_2). LC-MS (ESI) (m/z): 440 $[ML_2.2H_2O]^+$,422 $[ML_2.H_2O]^+$,404 $[ML_2]^+$,302 $[ML]^+$, 200 $[M]^+$.

ISSN- 2394-5125 VOL 07, ISSUE 10, 2020

2.6. DNA Binding Studies: The DNA bindingexperiment[15]was performed by Electronic absorption study,FluorescenceEmission study and Viscosity measurements.

2.6.1. Electronic Absorption spectroscopy: In this study, the DNA concentration per nucleotide was determined by using known molar extinction coefficient value of 6600 M^{-1} cm^{-1} at 260 nm. Absorption spectral titration of 180 µl µl Ni(II)-FSC complexes in TrisHCl buffer solution (pH 7.5) respectively have been performed by using fixed complex concentration to which increments of DNA stock solution ($25x10^{-6}$ µM) were added. After addition, the solution was allowed to incubate for 10 min before the absorption study was carried out.

2.6.2. Competitive binding fluorescence study: The aqueous solution of Ethidium Bromide shows very weak fluorescence, but in presence of DNA, it exhibit intense fluorescence due to intercalation to base pairs to DNA. So, 480 µl DNA was pretreated with 1620µl of TrisHCl buffer and 400 µl of Ethidium Bromide (EB) for 30 min. Ni(II)-FSC complexhas been added to the mixture and its effect on emission was measured. The emission was observed between 530-770 nm.

2.6.3. Viscosity measurements: Viscosity experiments were conducted on an Ostwald viscometer. The concentration of the Ni(II) complex of 50 µM introduced into CT-DNAsolution (200 µM) in TrisHCl buffer solution (pH 7.5) present in the viscometer. The sample was measured three times and average flow time was calculated. Viscosity values were calculated in the presence and absence of the complexes. The data were plotted as (η^1_{sp}/η_{sp}) Vs concentration of metal complex, where η^1_{sp} is the viscosity of DNA in presence of the complex and η_{sp} is the viscosity of CT-DNA alone.

2.7. Antimicrobial activity: The compounds synthesized were screened for their antibacterial activity against gram positive (B.subtilis) and gram negative (E. coli) bacteria at a concentration 50 µg/ml in DMSO by agar disc diffusion method[16]. The zone of inhibition is measured in mm.

3. Results and discussions:

3.1. FSC: The mass spectrum of FSC showed the molecular ion peak at m/z 103 $[M]^{+\cdot}$. The IR spectra showed all characteristic bands. The ^{1}H-NMR, D_2O exchangeable spectrum showed peaks mentioned in experimental part. ^{13}C-NMR showed two different peaks under different environment indicating keto-enol tautomerism. The electronic spectra revealed $n\rightarrow\pi^*$ transitions of both the C=O groups.

3.2. Computational studies of FSC: It has been observed from the spectral data of 1-formyl-3-semicabazide that the compound showed keto-enol tautomerism. Hence it is planned to construct all the possible tautomeric forms of FSC (Fig. 1) and studied for their energy parameters.

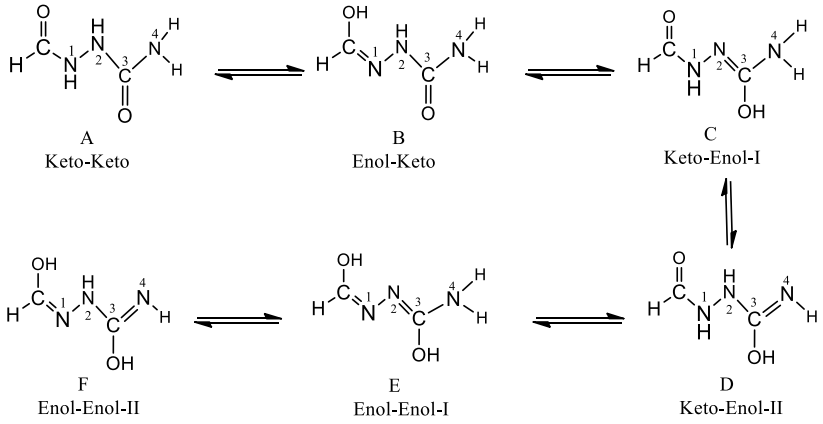

ISSN- 2394-5125 VOL 07, ISSUE 10, 2020

Fig. 1. Resonance structures of Keto-Enol Tautomers

Six forms of 1-formyl-3-semicarbazide (FSC)optimized geometries[17] were shown (Fig. 2) with atom numbering. The optimized geometry parameters- bond lengths, bond angles and dihedral angles for all six forms have been presented in the (Table. 1-6).

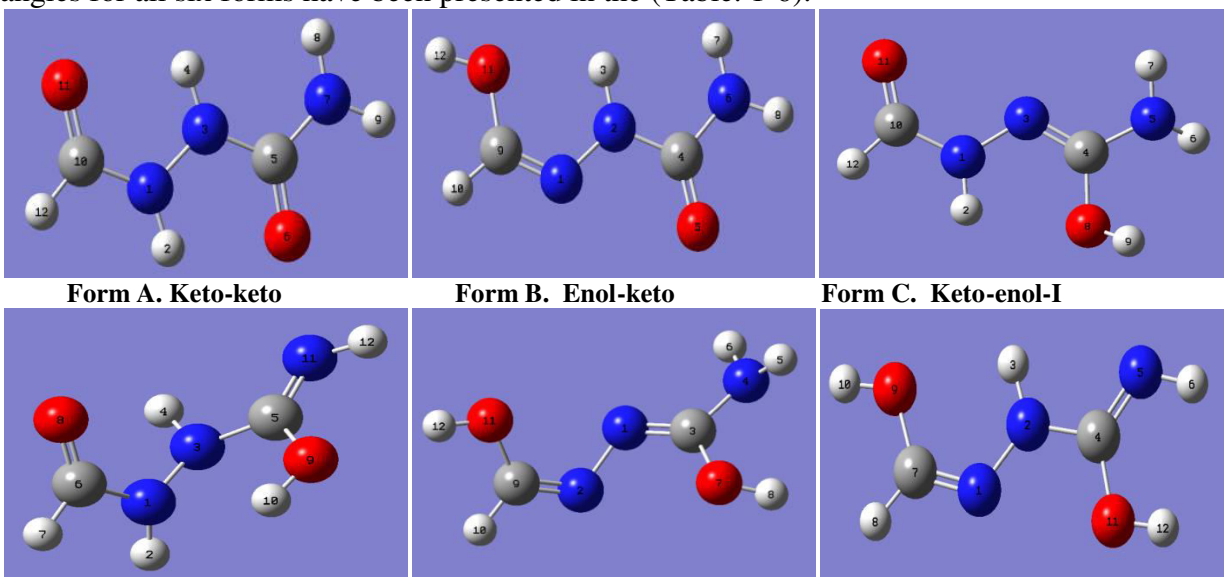

Form A. Keto-keto **Form B. Enol-keto** **Form C. Keto-enol-I**

Form D. Keto-enol-II **Form E. Enol-enol-I** **Form F. Enol-enol-II**

Fig. 2: Optimized geometry of six forms of FSC

Table. 1: Optimized geometric parameters of FSC – Form A

Bond Lengths (Å)		Bond Angles (°)		Dihedral Angles (°)	
R(1,2)	1.0102	A(2,1,3)	113.7737	D(2,1,3,4)	179.9405
R(1,3)	1.3995	A(2,1,10)	127.5912	D(2,1,3,5)	-0.3127
R(1,10)	1.351	A(3,1,10)	118.635	D(10,1,3,4)	0.0477
R(3,4)	1.0077	A(1,3,4)	113.9159	D(10,1,3,5)	179.7945
R(3,5)	1.3737	A(1,3,5)	117.2711	D(2,1,10,11)	180.0963
R(5,6)	1.2567	A(4,3,5)	128.8124	D(2,1,10,12)	0.0849
R(5,7)	1.3694	A(3,5,6)	120.5708	D(3,1,10,11)	-0.0275
R(7,8)	1.0036	A(3,5,7)	115.9612	D(3,1,10,12)	179.9611
R(7,9)	1.003	A(6,5,7)	123.468	D(1,3,5,6)	0.1875
R(10,11)	1.2516	A(5,7,8)	123.809	D(1,3,5,7)	-179.8405
R(10,12)	1.0919	A(5,7,9)	117.2035	D(4,3,5,6)	179.8905
		A(8,7,9)	118.9875	D(4,3,5,7)	-0.1376
		A(1,10,11)	122.6417	D(3,5,7,8)	0.1798
		A(1,10,12)	113.6294	D(3,5,7,9)	-179.9093
		A(11,10,12)	123.7289	D(6,5,7,8)	-179.8492
				D(6,5,7,9)	0.0617

Table. 2: Optimized geometric parameters of FSC – Form B

Bond Lengths (Å)		Bond Angles (°)		Dihedral Angles (°)	
R(1,2)	1.3786	A(2,1,9)	117.6502	D(9,1,2,3)	0.0053
R(1,9)	1.2758	A(1,2,3)	118.5468	D(9,1,2,4)	-179.9793
R(2,3)	1.0105	A(1,2,4)	119.6604	D(2,1,9,10)	-180.0135
R(2,4)	1.3956	A(3,2,4)	121.7927	D(2,1,9,11)	0.0104
R(4,5)	1.2397	A(2,4,5)	124.4752	D(1,2,4,5)	0.0434
R(4,6)	1.3803	A(2,4,6)	112.812	D(1,2,4,6)	-179.9644
R(6,7)	1.0037	A(5,4,6)	122.7127	D(3,2,4,5)	-179.9406
R(6,8)	1.0029	A(4,6,7)	124.3355	D(3,2,4,6)	0.0515
R(9,10)	1.078	A(4,6,8)	116.8985	D(2,4,6,7)	0.0978

ISSN- 2394-5125 VOL 07, ISSUE 10, 2020

R(9,11)	1.402	A(7,6,8)	118.766	D(2,4,6,8)	-179.9611
R(11,12)	0.9695	A(1,9,10)	120.0177	D(5,4,6,7)	-179.9099
		A(1,9,11)	121.4331	D(5,4,6,8)	0.0312
		A(10,9,11)	118.5493	D(1,9,11,12)	-179.844
		A(9,11,12)	113.2146	D(10,9,11,12)	0.1795

Table. 3: Optimized geometric parameters of FSC – Form C

Bond Lengths (Å)		Bond Angles (°)		Dihedral Angles (°)	
R(1,2)	1.0121	A(2,1,3)	118.5009	D(2,1,3,4)	-4.769
R(1,3)	1.3936	A(2,1,10)	120.2584	D(10,1,3,4)	176.8393
R(1,10)	1.3704	A(3,1,10)	121.2211	D(2,1,10,11)	-179.5474
R(3,4)	1.282	A(1,3,4)	117.004	D(2,1,10,12)	0.4982
R(4,5)	1.3829	A(3,4,5)	122.8122	D(3,1,10,11)	-1.1837
R(4,8)	1.4018	A(3,4,8)	121.7097	D(3,1,10,12)	178.8619
R(5,6)	1.0086	A(5,4,8)	115.4636	D(1,3,4,5)	-170.9384
R(5,7)	1.0069	A(4,5,6)	118.4786	D(1,3,4,8)	7.6127
R(8,9)	0.9734	A(4,5,7)	115.4028	D(3,4,5,6)	-133.0851
R(10,11)	1.2356	A(6,5,7)	115.5447	D(3,4,5,7)	10.1121
R(10,12)	1.0994	A(4,8,9)	111.6826	D(8,4,5,6)	48.2802
		A(1,10,11)	126.9357	D(8,4,5,7)	-168.5227
		A(1,10,12)	110.4477	D(3,4,8,9)	-149.45
		A(11,10,12)	122.6166	D(5,4,8,9)	29.2012

Table. 4: Optimized geometric parameters of FSC – Form D

Bond Lengths (Å)		Bond Angles (°)		Dihedral Angles (°)	
R(1,2)	1.0107	A(2,1,3)	115.91	D(2,1,3,4)	100.5418
R(1,3)	1.3954	A(2,1,6)	118.7172	D(2,1,3,5)	-109.7349
R(1,6)	1.3885	A(3,1,6)	121.9396	D(6,1,3,4)	-58.2584
R(3,4)	1.009	A(1,3,4)	117.5482	D(6,1,3,5)	91.4649
R(3,5)	1.4054	A(1,3,5)	120.6071	D(2,1,6,7)	14.2844
R(5,9)	1.3867	A(4,3,5)	115.0578	D(2,1,6,8)	-166.3759
R(5,11)	1.2689	A(3,5,9)	115.0361	D(3,1,6,7)	172.5138
R(6,7)	1.0972	A(3,5,11)	119.8297	D(3,1,6,8)	-8.1465
R(6,8)	1.2306	A(9,5,11)	125.0789	D(1,3,5,9)	16.0622
R(9,10)	0.9759	A(1,6,7)	111.7711	D(1,3,5,11)	-166.5064
R(11,12)	1.0177	A(1,6,8)	124.6594	D(4,3,5,9)	166.4941
		A(7,6,8)	123.566	D(4,3,5,11)	-16.0745
		A(5,9,10)	112.0631	D(3,5,9,10)	-8.3011
		A(5,11,12)	114.8445	D(11,5,9,10)	174.4219
				D(3,5,11,12)	-177.4618
				D(9,5,11,12)	-0.3058

Table. 5: Optimized geometric parameters of FSC – Form E

Bond Lengths (Å)		Bond Angles (°)		Dihedral Angles (°)	
R(1,2)	1.4116	A(2,1,3)	117.6815	D(3,1,2,9)	128.8811
R(1,3)	1.2816	A(1,2,9)	118.3431	D(2,1,3,4)	163.4713
R(2,9)	1.274	A(1,3,4)	121.6553	D(2,1,3,7)	-16.9098
R(3,4)	1.3857	A(1,3,7)	123.6965	D(1,2,9,10)	173.9177
R(3,7)	1.3925	A(4,3,7)	114.6472	D(1,2,9,11)	-6.9569
R(4,5)	1.0077	A(3,4,5)	118.4825	D(1,3,4,5)	136.0074
R(4,6)	1.0062	A(3,4,6)	115.4966	D(1,3,4,6)	-8.0546
R(7,8)	0.9747	A(5,4,6)	115.9168	D(7,3,4,5)	-43.6438
R(9,10)	1.0819	A(3,7,8)	111.0139	D(7,3,4,6)	172.2942
R(9,11)	1.3896	A(2,9,10)	118.2306	D(1,3,7,8)	147.5784
R(11,12)	0.9717	A(2,9,11)	124.734	D(4,3,7,8)	-32.7786

ISSN- 2394-5125 VOL 07, ISSUE 10, 2020

		A(10,9,11)	117.0299	D(2,9,11,12)	178.0613
		A(9,11,12)	111.7334	D(10,9,11,12)	-2.8038

Table. 6: Optimized geometric parameters of FSC – Form F

Bond Lengths (Å)		Bond Angles (°)		Dihedral Angles (°)	
R(1,2)	1.3763	A(2,1,7)	117.5841	D(7,1,2,3)	0.0203
R(1,7)	1.2776	A(1,2,3)	120.8722	D(7,1,2,4)	-180.0062
R(2,3)	1.0097	A(1,2,4)	122.6291	D(2,1,7,8)	-180.0003
R(2,4)	1.376	A(3,2,4)	116.4987	D(2,1,7,9)	0.0102
R(4,5)	1.2846	A(2,4,5)	119.1149	D(1,2,4,5)	-179.9697
R(4,11)	1.3906	A(2,4,11)	111.9758	D(1,2,4,11)	0.0264
R(5,6)	1.0188	A(5,4,11)	128.9092	D(3,2,4,5)	0.0048
R(7,8)	1.078	A(4,5,6)	116.3244	D(3,2,4,11)	-179.999
R(7,9)	1.3988	A(1,7,8)	119.8057	D(2,4,5,6)	-179.983
R(9,10)	0.9693	A(1,7,9)	121.4904	D(11,4,5,6)	0.0216
R(11,12)	0.9721	A(8,7,9)	118.7039	D(2,4,11,12)	179.9844
		A(7,9,10)	113.3097	D(5,4,11,12)	-0.02
		A(4,11,12)	110.6274	D(1,7,9,10)	-179.9081
				D(8,7,9,10)	0.1022

Thermochemical properties: Thermochemical properties like total energy, entropy, free energy, heat capacity, dipole moment, electronic energies of all the forms of FSC were presented in the Table. 7. It has been observed that form A, C and E are more reactive as form A shows less free energy value, form C exhibits low entropy and high dipole momentvalues, while form E shows high enthalpy.

Table. 7: Thermochemical properties of 1-formyl-3-semicarbazide derivatives

Properties	Form A	Form B	Form C	Form D	Form E	Form F
Partial charge	0.00e	0.00e	0.00e	0.00e	0.00e	0.00e
Total energy (Kcal/mol)	56.42566	55.77368	55.95189	55.98264	55.09283	55.24657
Entropy(Kcal/mol-deg)	0.08542	0.08634	0.08366	0.08416	0.08600	0.08482
Enthalpy (Kcal/mol)	-247111.2	-247094.0	-247088.5	-247085.3	-247069.1	-247071.3
Free energy (Kcal/mol)	-247140.1	-247123.5	-247117.2	-247114.2	-247098.5	-247100.4
Heat capacity (Kcal/moldeg)	0.02586	0.02648	0.02592	0.02500	0.02684	0.02614
Dipole moment	2.23644	6.32527	6.74889	5.23133	1.69488	1.93762
RMS gradient (Kcal/mol)	0.01570	0.00766	0.00868	0.00829	0.01141	0.00841
Electronic energy (Kcal/mol)	-247176.4	-247158.9	-247153.4	-247150.2	-247133.3	-247135.6

Table. 8: Quantum Chemical descriptors of FSC: A-F

Parameters(eV)	Form A	Form B	Form C	Form D	Form E	Form F
E_{HOMO}	-0.23731	-0.23570	-0.22525	-0.25455	-0.21521	-0.21983
E_{LUMO}	-0.00427	-0.00207	-0.00947	-0.03293	+0.00454	-0.00058
ΔE_{gap}	0.23304	0.23363	0.21578	0.22162	0.21975	0.21925
IE	0.23731	0.23570	0.22525	0.25455	0.21521	0.21983
EA)	0.00427	0.00207	0.00947	0.03293	-0.00454	0.00058
μ	-0.12079	-0.11888	-0.11736	-0.14374	-0.10533	-0.11020

ISSN- 2394-5125 VOL 07, ISSUE 10, 2020

χ	0.12079	0.11888	0.11736	0.14374	0.10533	0.11020
η	0.11652	0.11681	0.10789	0.11081	0.10987	0.10962
S	8.58221	8.56091	9.26869	9.02445	9.10166	9.12242
ω	0.06261	0.06048	0.06382	0.09322	0.05046	0.05537

FSC	**HOMO**	**ΔE_{gap} (eV)**	**LUMO**
Form A.	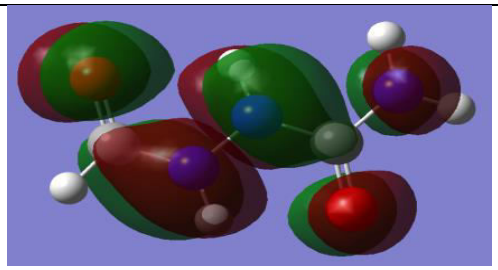	0.23304	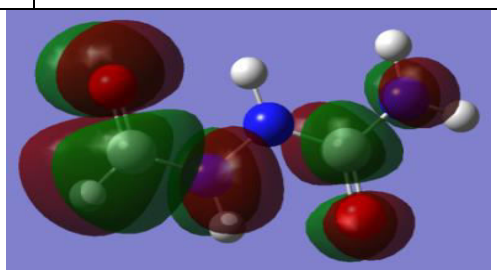
Form B.	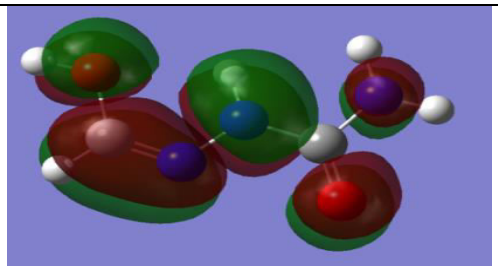	0.23363	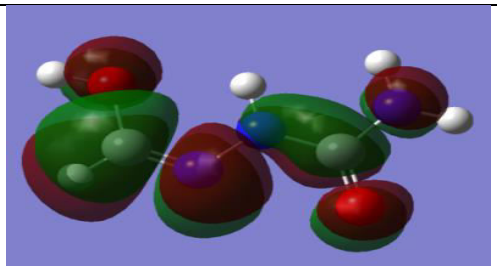
Form C.	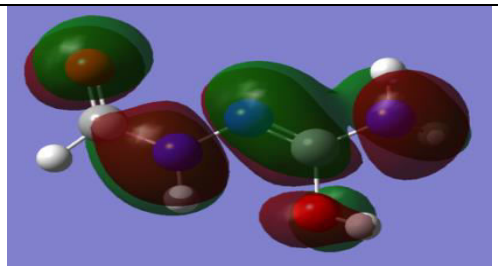	0.21578	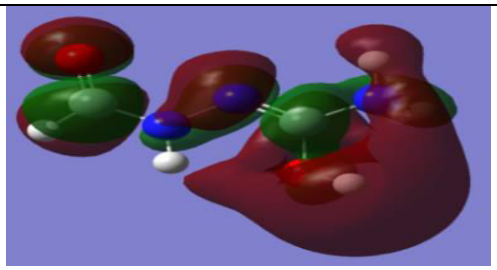
Form D.	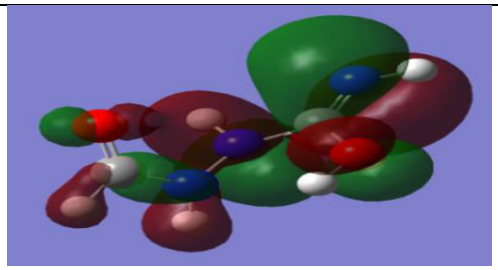	0.22162	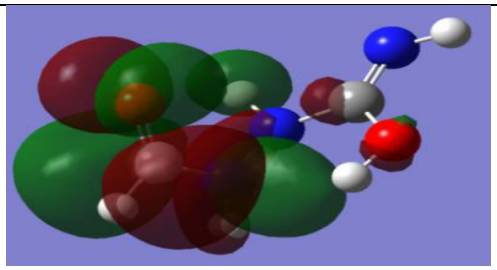
Form E.	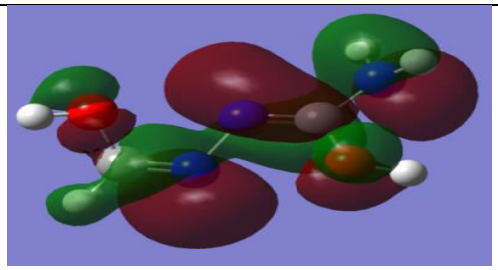	0.21975	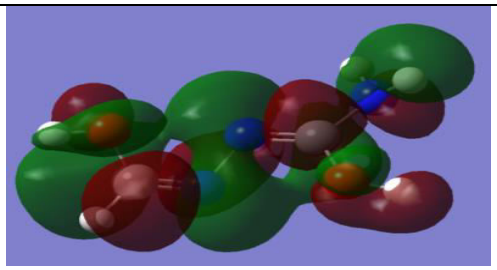

ISSN- 2394-5125 VOL 07, ISSUE 10, 2020

Form F.	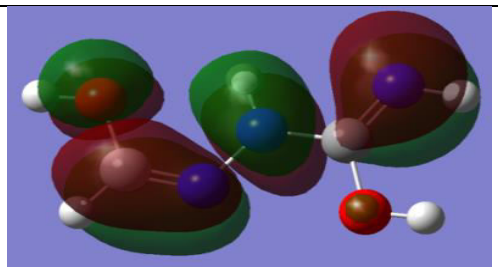	0.21925	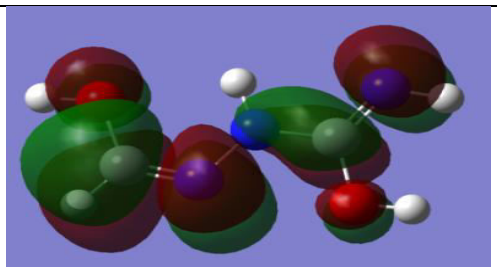

Fig. 3: HOMO-LUMO orbitals of FSC in various tautomeric forms and the energy gaps

FMO: The frontier molecular orbitals HOMO and LUMO surfaces were generated of FSC (A-F) with DFT- RB3LYP with basis set of 6-311G (d,p) has been presented in Figure 3. From energies of FMO (E_{HOMO}, E_{LUMO}), ΔEgap, electronegativity (χ), chemical potential (μ), global hardness (η), global softness (S) and global electrophilicity index (ω)[18-23]for six forms of FSC were calculated and tabulated in the Table. 8.

From the Table. 8 of all tautomers of FSC, it has been observed that the low energy gaps in all the forms indicating the possibility of electronic excitation easily. The lowest energetic gap was in the form C: keto-enol-I (ΔEgap). Its lowest value reveals its more softness and the highest energy gap is observed in form B (ΔEgap) slightly hard molecule. The enol-enol-I (form E) has highest HOMO energy, which makes it an electron donor. Enol-enol -II (form F) has lowest LUMO energy revealing this form as electron acceptor. IP and EA are important in calculating the E.N (χ) and global hardness (η), which are in turn related to HOMO and LUMO one electron orbital energies respectively. Enol-enol-I (form E) has lowest IP value and will be better electron donor.keto-enol -II (form D) showed large EA value (A) hence acts as electron acceptor. The structure of the molecule will vary the chemical reactivity. The global hardness of keto-enol-I (form C) (η) was lowest of all and its softness value (S) has been greater among all the forms of FSC. Thus form C can be predicted to be more reactive than others.Keto-enol -II (form D) possesses higher E.N value (χ) than other forms, it is best electron acceptor which is also supported by its EA value. The value of electrophilicity (ω) for form D showed its strong electrophilicity. Form C showed lower ΔEgap, hence it acts as a soft molecule showing high chemical reactivity, low kinetic stability and will be more polarizable.

Molecular electrostatic potential mapping(MEP): From MEP[24, 25] mapping of all forms of FSC (Fig.4) it has been observed that the red regionaround oxygen and nitrogen atoms with amide linkages indicates more negative electrostatic potential, which reveal that these sites were more susceptible to electrophillic attack[26-29].Mulliken charges on the atoms of all the keto-enol forms of FSC were recorded and presented in the table. 9. The net charges on the molecular forms have been found to be zero. The charges were also presented on the atoms in the MEP mapping (Fig. 7).

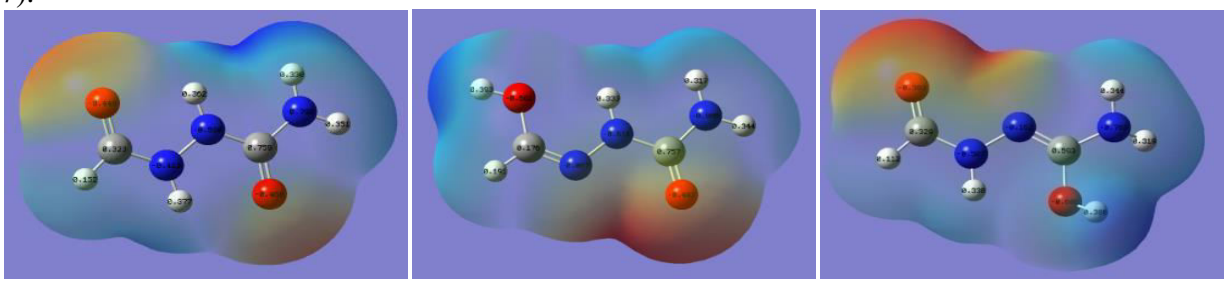

Form A. Keto-keto **Form B. Enol-keto** **Form C. Keto-enol-I**

ISSN- 2394-5125 VOL 07, ISSUE 10, 2020

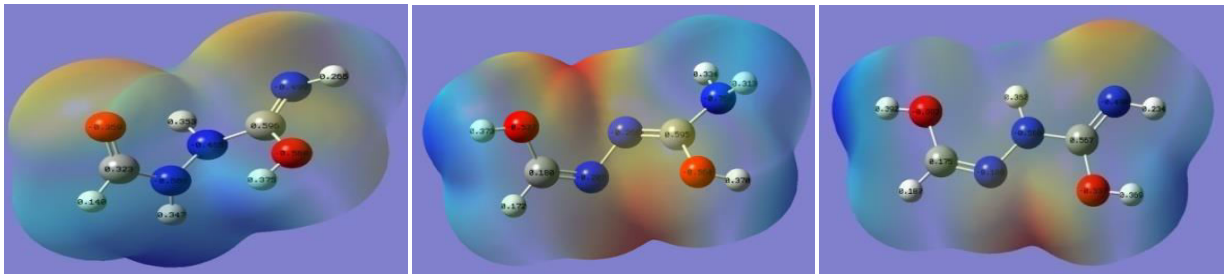

Form D. Keto-enol-II Form E. Enol-enol-I Form F. Enol-enol-II

Fig. 4: Molecular Electrostatic potential mapping of FSC

Table. 9: Mulliken charges on the atoms A-F of 1-formyl-3-semicarbazide derivatives

Form A	Form B	Form C	Form D	Form E	Form F
1 N -0.396169	1 N -0.086834	1 N -0.507332	1 N -0.509399	1 N -0.268528	1 N -0.189186
2 H 0.336378	2 N -0.616155	2 H 0.338221	2 H 0.347183	2 N -0.207339	2 N -0.473513
3 N -0.452768	3 H 0.332933	3 N -0.161590	3 N -0.464833	3 C 0.594995	3 H 0.329038
4 H 0.336442	4 C 0.757252	4 C 0.593289	4 H 0.352962	4 N -0.760320	4 C 0.544566
5 C 0.488801	5 O -0.401937	5 N -0.763052	5 C 0.595993	5 H 0.312936	5 N -0.491470
6 O -0.337191	6 N -0.805891	6 H 0.319031	6 C 0.322919	6 H 0.333685	6 H 0.245295
7 N -0.700664	7 H 0.316898	7 H 0.344112	7 H 0.140449	7 O -0.563972	7 C 0.197005
8 H 0.325153	8 H 0.344103	8 O -0.606152	8 O -0.358624	8 H 0.369850	8 H 0.200814
9 H 0.329321	9 C 0.175805	9 H 0.385844	9 O -0.568020	9 C 0.179764	9 O -0.547003
10 C 0.232136	10 H 0.191307	10 C 0.328663	10 H 0.375373	10 H 0.172235	10 H 0.373293
11 O -0.328437	11 O -0.600589	11 O -0.382645	11 N -0.499042	11 O -0.536660	11 O -0.558420
12 H 0.166999	12 H 0.393107	12 H 0.111611	12 H 0.265039	12 H 0.373353	12 H 0.369581

3.3. Equilibrium studies:

The pKa value has been obtained from the titration plots (Fig.5) and linear plot (Fig.6, Table-10) of Log (1- $\bar{n}_A$)/ $\bar{n}_A$as a function of pH was 8.84, revealing FSC to be a monobasic acid. The $\bar{n}$ values[30] obtained from the curves were in the range of 0.222 to 0.931revealing the formation of1:1 Ni(II)-FSC compex.complexes in the solution (Table.11), the linear plots of Log (1- $\bar{n}$) / $\bar{n}$ Vs pL have been plotted in (Fig.10) and the stability constants were obtained as Log K_1–5.088.

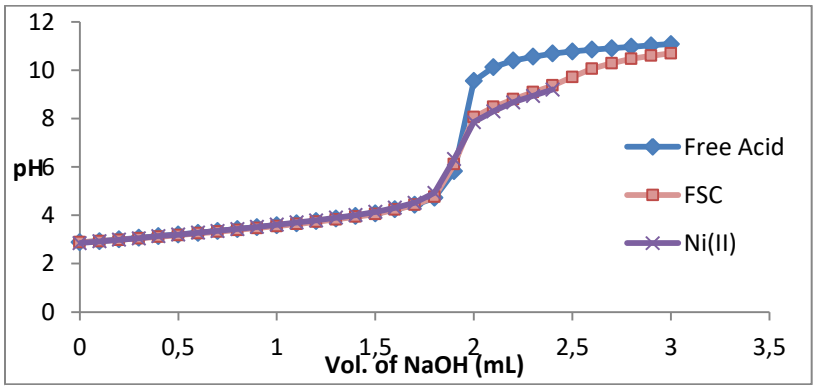

Fig. 5: pH titration curves of M(II)-FSC binary system in 70% v/v DMF-water medium at 303K and 0.1 M ionic strength.

Table 10. Data for obtaining dissociation constants of FSC in 70% v/v DMF-water medium at 303K and 0.1M ionic strength.

pH	$\bar{n}_A$	Log(1-$\bar{n}_A$) / $\bar{n}_A$
8.4	0.75	-0.48
8.5	0.69	-0.35

ISSN- 2394-5125 VOL 07, ISSUE 10, 2020

8.6	0.65	-0.27
8.7	0.59	-0.16
8.8	0.52	-0.03
8.9	0.47	0.05
9.0	0.41	0.16
9.1	0.35	0.27
9.2	0.29	0.39

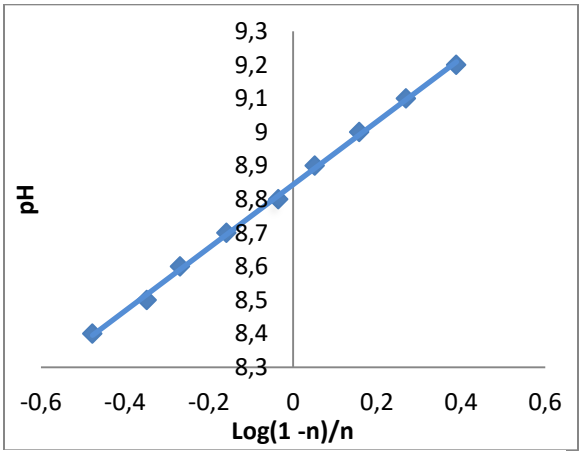

Fig. 6. Plot of Log(1- $\bar{n}_A$)/ $\bar{n}_A$ Vs pII of FSC in 70% v/v DMF-water medium

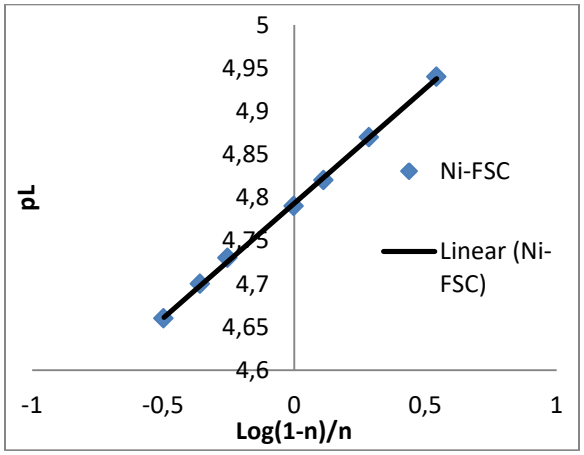

Fig. 7. Plot of Log(1-n)/n Vs pL of Ni(II)-FSC in 70% v/v DMF-water medium

Table 11. Data for obtaining formation curves of Ni(II)-FSC in 70% v/v DMF-water medium at 303K and 0.1M ionic strength

$\bar{n}$	Log(1-$\bar{n}$)/$\bar{n}$	pL
0.931	-1.13	4.68
0.796	-0.59	4.87
0.683	-0.33	4.96
0.556	-0.1	5.05
0.455	0.08	5.12
0.341	0.29	5.19
0.222	0.54	5.29

3.4. Characterization of metal complexes a and b: The metal complexes **a** and **b** of FSC (Scheme) were amorphous, non-hygroscopic, stable at room temperature, and were soluble in DMSO and DMF.Mass spectra of the complex**a**revealed it to be in 1:1 [M:L] composition and complex **b**showed1:2 [M:L] composition.Volhard's test showed negative result for the chloride ion. Molar conductance of the complexes was recorded in DMSO suggested their non-electrolytic nature. The physical data of the M(II)-FSC complexes have been presented in Table. 12.

Table-12. Physical constants and Analytical Data of M(II)-FSC complexes

S.No	Compound/ Molecular formula	Colour	M.P °C	Analysis Found (Calc)%		
				C	H	N
1.	FSC	Off White	182- 185	23.30 (23.30)	4.89 (4.85)	40.76 (40.77)

ISSN- 2394-5125 VOL 07, ISSUE 10, 2020

2.	$[NiL(H_2O)_2]_n.nH_2O$	Pale Blue	DP	12.27 (12.25)	3.60 (3.60)	21.46 (21.45)
3.	$[HgL_2(H_2O)_2]$	White	DP	10.90 (10.90)	2.74 (2.74)	19.07 (19.09)

3.4.1. Vibrational spectra: The IR spectrum of the cobalt(II) complex of FSC(Fig. 8) has been compared with the ligand spectrum to learn the changes in the peak positions upon complexation. The ligand spectral peak corresponding to asymmetric and symmetric stretch of NH_2 at 3186 cm^{-1} and3155 cm^{-1}, observed a shift to higher frequencywith a peak at 3196 cm^{-1}, the absence of other peak indicates the binding of N(4) atom. Similarly the $\upsilon_{N2\text{-}H}$ peak has increasedfrom 3020 $cm^{-1}$to 3030 cm^{-1}showed N(2) bindingto Co(II) ionwithout deprotonation. Further $\upsilon_{N1\text{-}H}$ peak at 3091 $cm^{-1}$of the ligand disappeared in the IR spectrum of the complex revealing the involvement of N(1) on complexation. The υ_{CONH} (1695cm^{-1}) appeared in the ligand spectrum showed shift towards lower frequency 1616 cm^{-1} in the metal complex indicating binding of oxygen to the metal ion in keto form. The binding of all the four sites to a single metal ion may result in the strain in the complex, therefore two sites N_2 and 'O'(formyl C=O) coordinate with one metal ion and the other two sites N(1) and N(4) coordinate with another metal ion resulting in five membered chelate polymeric complex. The formation of new bands in the region 600-500 cm^{-1}, 440-410 cm^{-1} and 410-350 cm^{-1} may be attritubed $\upsilon_{M\text{-}N}$, $\upsilon_{M\text{-}OH2}$ and $\upsilon_{M\text{-}O}$bonds respectively.

IR spectrum of Mercury(II)-FSC complex (Fig. 9), $\upsilon_{N1\text{-}H}$peakwas shifted to higher wavelength at 3138 cm^{-1}. The $\upsilon_{N2\text{-}H}$peak disappeared on complexation, also theformyl υ_{CO} peak appeared at less frequency (1606 cm^{-1}) revealingthe binding of N(2) andformyl oxygenwith metal ion. As a result Hg(II) ion coordinate with the two potential donor sites [formyl oxygen and N(2) nitrogen] forms a five membered chelate complex. The peaks corresponding to $\upsilon_{M\text{-}N}$, $\upsilon_{M\text{-}OH2}$and$\upsilon_{M\text{-}O}$ bonds were also observed.

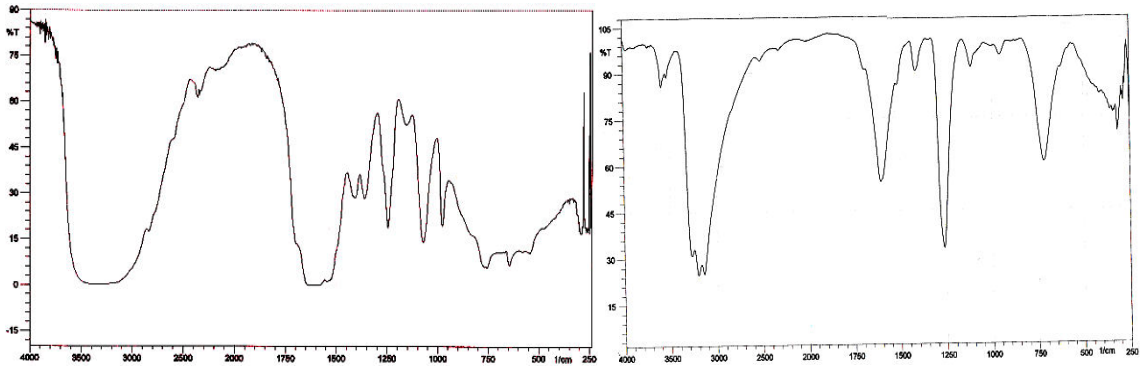

Fig. 8: IR spectrum of Ni(II)-FSC complex Fig. 9: IR spectrum of Hg(II)-FSC complex

3.4.2. Electronic spectra: The transitions observed in the UV –Visible spectrum of Ni(II)-FSC complex (Fig.10) were$^3A_{2g}$ (F) → $^3T_{2g}$ (F) at 13131 cm^{-1}(762 nm)(υ_1), $^3A_{2g}$ (F) → $^3T_{1g}$ (F) 15923 cm^{-1} (628 nm) (υ_2) and $^3A_{2g}$ (F) → $^3T_{1g}$ (P) 26385 cm^{-1} (379 nm) (υ_3), confirming its octahedral geometry[31, 32].

ISSN- 2394-5125 VOL 07, ISSUE 10, 2020

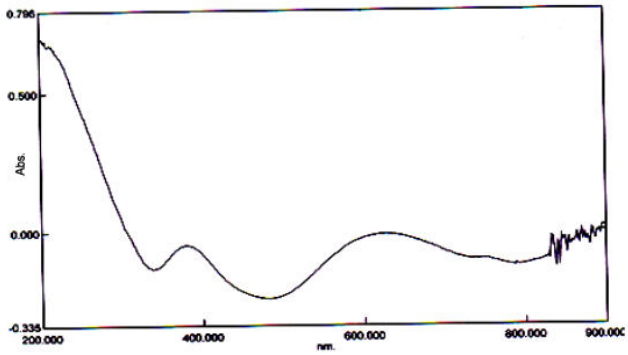

Fig. 10: Electronic spectrum of Ni(II)-FSC complex

Table-13. Electronic spectral data of FSC and its complexes

Compound	Absorption Bands cm^{-1}	Band assignment	υ_2/υ_1	B' (cm^{-1})	10Dq (cm^{-1})	β
FSC	45351 46403	$n\rightarrow\pi^*$ (C=O) $n\rightarrow\pi^*$ (C=O)	-	-	-	-
Ni(II)-FSC	13131 15923 26385	$^3A_{2g}$ (F) → $^3T_{2g}$ (F) $^3A_{2g}$ (F) → $^3T_{1g}$ (F) $^3A_{2g}$ (F) → $^3T_{1g}$ (P)	5.08	194.33	13131	0.179

3.4.3. ESR: In the ESR spectra of Ni(II)-FSC (Fig.11) complex $g_{\parallel} > g_{\perp}$indicates the presence of unpaired electronin the $d_{x^2-y^2}$ orbital suggesting its tetragonally distorted octahedral geometry[33]of the M(II)-FSC complexes.For Ni(II)-FSC complex G > 4, revealing negligible exchange interactions.The λ value has been calculated using the electronic transition energy ($^3A_{2g}$ (F) → $^3T_{2g}$ (F) of 13131cm^{-1}).The calculated λ values for Ni(II)-FSC complex is 211, which isless than that of free M(II) ion. This reduction in λ from the free ion value is an evidence of covalence in M-L bond[34]. The calculated α^2 value[35] found to be less than one, indicating the covalent character , further β^2, γ^2(bonding parameters) and orbital reduction factors$K_{\parallel}^2$ and $K_{\perp}^2$($K > K_{\parallel}^2$, $K_{\perp}^2$) (Table.14) contributing more for out-of-plane π-bonding than in-plane π-bonding.

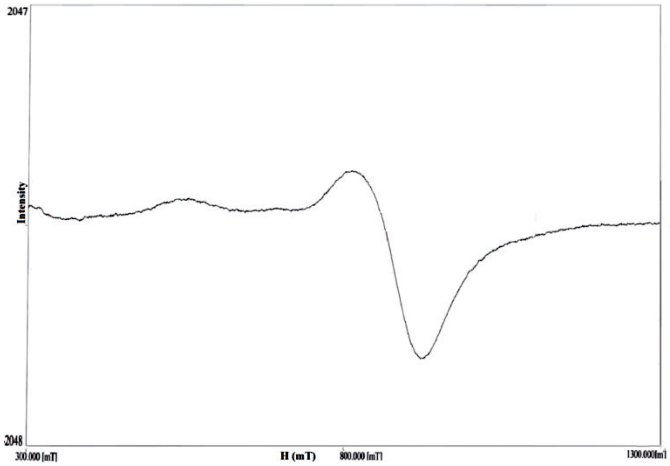

Fig. 11. ESR spectrum of Ni(II)-FSC complex

Table. 14 . Spin Hamiltonian parameters of M(II)-FSC complexes

ISSN- 2394-5125 VOL 07, ISSUE 10, 2020

Complex	$g_{\|}$	$g_{\perp}$	G	$A_{\|}$	α^2	β^2	γ^2	$K_{\|}^2$	$K_{\perp}^2$
Ni(II)-FSC	2.1318	2.0304	4.6070	0.0071	0.3788	1.7264	1.4999	0.5307	0.1194

3.4.4. Thermogravimetric Analysis: The Thermal decomposition curve of Ni(II)-FSC (Fig. 12a) showed in itsfirst decomposition stepupto 110°C, loss of 6.67% of complex,due to the evaporation of lattice water molecule.In the next decomposition step upto 190°C showedthe loss of 14.22% weight due to loss of two coordinated water molecules. Further sudden and steep weight loss of the complex in the next two steps upto 600ºC and gradual decomposition up to 1000ºC indicates decomposition of organic moiety of the complex. The remaining residue of 29.85% weight corresponds to NiOin 1:1 ML ratio of metal complex.

In Hg(II)-FSC complex thermogram (Fig.12 b), it has been observed that the weight loss of 7.14% up to 230ºC corresponds to the loss of two moles of coordinated water. Further complete decomposition was observed up to 1000 ºC.

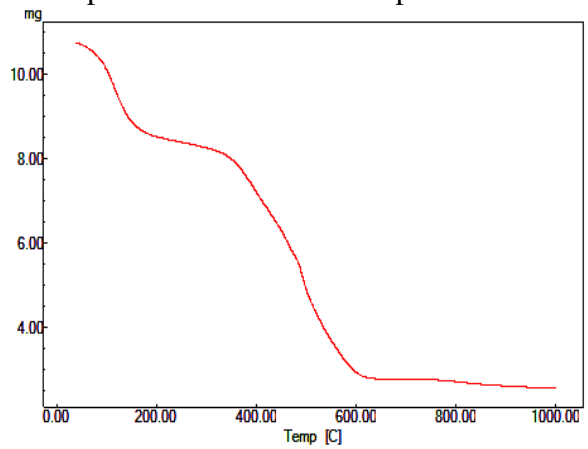

Fig. 12a: Thermogram of Ni(II)-FSC complex

Fig. 12b: Thermogram of Hg(II)-FSC complex

3.4.5. ^{1}H-NMR: The ^{1}HNMR spectrum of Hg(II)-FSC chelate (Fig.13) peak of the 2° amides (N(2)H) group observed in the ligand at δ7.40 ppm was not absent, indicating loss of one proton upon complexation**.**

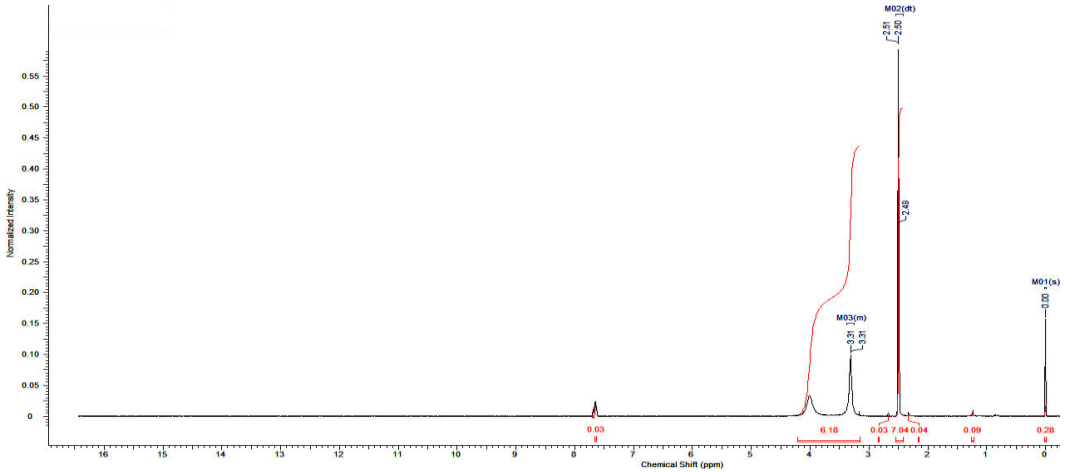

Fig. 13: ^{1}H-NMR spectrum of Hg(II)-FSC complex

ISSN- 2394-5125 VOL 07, ISSUE 10, 2020

3.5. DNA binding studies: The binding interaction of Ni(II)-FSC complex with calf-thymus DNA has been investigated with the help of spectroscopic[36] (Electronic Absorption and Fluorescence measurements) and viscosity measurements.

3.5.1. DNA-Binding -Electronic Absorption Study: In the electronic spectra of Ni(II)-FSC complex (Fig.14) a strong absorption peak at 274 nm was observed with the decrease in absorption intensity (hypochromism) after addition of DNA, which indicates the strong interactions between DNA and the complex may be because of smaller and planar nature due to resonance. A minor red shift was observed along with hypochromism[37]revealing the intercalation mode of binding.In the plot of [DNA] / (ε_a-ε_f) versus [DNA], the ratio of the slope to intercept gives the value of K_b. The K_b value (Fig.17 inset) for Ni(II)-FSC complex was estimated as 1.1951 x $10^3 M^{-1}$.

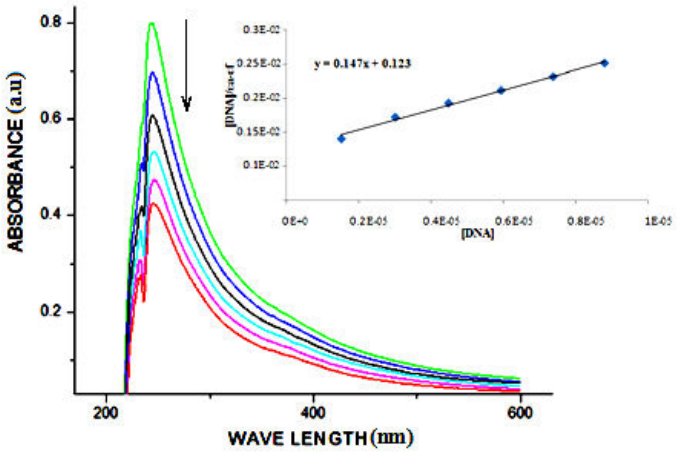

Fig.14: Electronic spectra of Ni(II)-FSC (K_b=1.1951 x $10^3 M^{-1}$) (Inset: plot of [DNA]/(ε_a-ε_f) Vs [DNA]

3.5.2. Competitive binding fluorescence study: Ethidium bromide (EB) intense fluorescence light in the presence of DNA, due to its strong intercalation between the adjacent base pairs.The quenching of EB bound DNA by Ni(II)-FSC complex (Fig.15) was in good agreement with the linear Stern-Volmer equation, which also indicates that the complex binds to DNA[38]. In the plot of I_0 / I versus [complex] / [DNA], K_{sv} is given by the ratio of the slope to intercept.The K_{sv} valuefor complex a has been calculated as 0.11818 X 10^3 M^{-1}

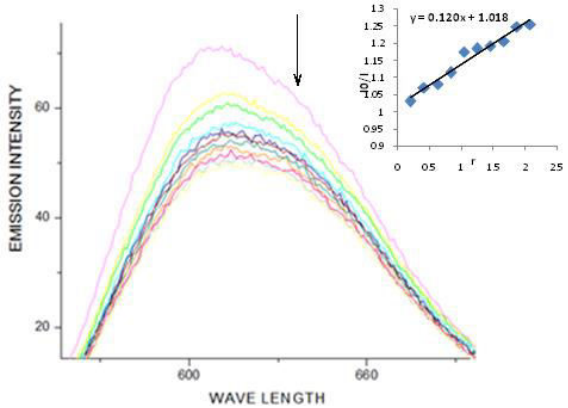

Fig. 15: Emission spectra of Ni(II)-FSC(K_{SV}=0.11818 X 10^3 M^{-1})

ISSN- 2394-5125 VOL 07, ISSUE 10, 2020

3.5.3. Viscosity measurements: The binding of DNA with the Ni(II)-FSC complex (Fig. 16) was carried out by viscosity measurements. The data obtained was presented as $(\eta/\eta_0)^{1/3}$Vs the concentration of metal complexes, where η is the viscosity of DNA in presence of complexes and η_0 is the viscosity of DNA alone. It was observed that the complex interact with DNA by intercalation between DNA base pairs due to lengthening of DNA helix.

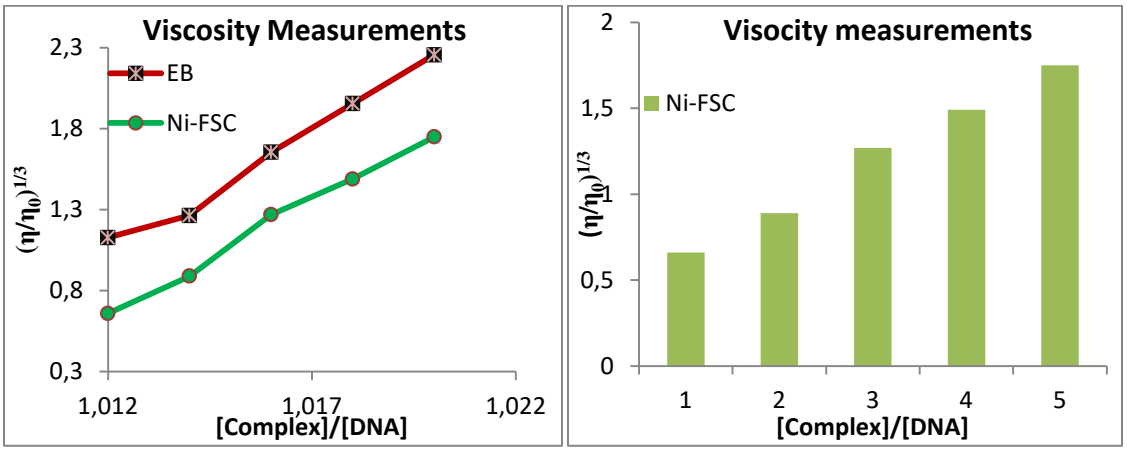

Fig. 16: Effect of increasing concentrations of EtBr (red line), Ni(II)-FSC (green line), on the relative viscosity of CT-DNA

3.6.Antimicrobial activity:FSC and its metal chelates a and b were screened for antimicrobial activity against bacterial strains of *Escherichia coli* (gram negative), and *Bacillus subtilis* (gram positive) for antibacterial activity, at a concentration of 50µg/ml of DMSO and gentamycin as a standard[39]. FSC and the complex a (Table. 15) showed activity against gram negative and gram positive bacteria, while complex b showed activity only for *E.coli*.

Table.15: Anti microbial activity of metal complexes

Sample	Escherichia coli	Bacillus subtilis
FSC	28mm	16mm
Ni(II)-FSC	19mm	10mm
Hg(II)-FSC	21mm	-

3.7. Conclusions: IR spectra predicted the binding sites. Computational studies used to optimize the geometry of the molecule and the HOMO-LUMO calculations carried using DFT confirms transfer of charge within the molecule. Equilibrium studies revealed the formation of only 1:1 metal complexes of Ni(II) ion with FSC in solution. The formation of 1:1 solid Ni(II)-FSC complex has been supported by mass spectra, TGA and equilibrium studies. DNA binding studies reveal that the Ni(II)-FSC complex effectively bind with DNA by intercalation mode. FSC showed higher antibacterial activity against *E. coli* ad *B.subtilis* than complexes **a** and **b**. Complex **b** was resistant to gram positive bacteria.

ISSN- 2394-5125 VOL 07, ISSUE 10, 2020

References:

[1] SS Rollas and S. Gunizkucukguzet, *Biological activities of Hydrazone Derivatives, Molecules*. 12 (2007) 1910-1939. https://doi.org/10.3390/12081910
[2] M.M. Omar, G.G. Mohamed, A.A. Ibrahim, Spectroscopic characterization of metal complexes of novel Schiff base. Synthesis, thermal and biological activity studies. *Spect. Chimi. Acta* Part A, 73 (2009)358-369.https://doi.org/10.1016/j.saa.2009.02.043
[3] G Schwarzenbach., Complexometric Titrations. Interscience, New York. 1952: A. I. Vogel., "*A Textbook of Quantitative Inorganic Analysis*" (1952) ELBS, London. https://doi.org/10.1021/ed029p319.1
[4] A. M. Vijesh, M. IsloorArun, SandeepTelkar, M. Arulmoli, Hoong-Kun Fun.;*Arabian Journal of Chemistry*, (2013) 6, 197-204.https://doi.org/10.1016/j.arabjc.2011.10.007.
[5] N. Raman and J. Dhaveethu Raja; *Indian Journal of Chemistry,* vol.46 A, (2007) 1611-1614, http://dx.doi.org/10.4067/S0717-97072007000200004
[6] B. Sireesha, Ch. Sarala Devi and P. Raghavaiah; *Indian Journal of Chemistry*, (2008) 47B 592-596.
[7] Burkhard Miehlich, Andreas Savin, Hermann Stoll and Heinzwerner Preussg, ,"Result obtained with the correlation energy Density Functionals of Becke and Lee, Yang and Parr, J. *Chemical physics Letters*, (1989)Volume 157, pp 200-206.
https://ui.adsabs.harvard.edu/link_gateway/1989CPL...157..200M/doi:10.1016/0009-2614(89)87234-3
[8] Axel D. Becke, Density-functional thermochemistry. III. The role of exact exchange, *J. Chem. Phys*. (1993), Vol 98 (7), pp 5648- 5652. https://doi.org/10.1063/1.464913
[9] Rajalakshmi, Divya., Analysis of Highest Occupied and Lowest Unoccupied Molecular Orbital on Harmaline. *International Journal of Current Research and Review* (2018), vol.10, Issue 21. http://dx.doi.org/10.31782/IJCRR.2018.3235
[10] J. F. Janak, "Proof that $\delta E\delta ni=\varepsilon in$ density-functional theory,"*Physical Review B*, vol. 18, no. 12, pp. 7165–7168, 1978.https://doi.org/10.1103/PhysRevB.18.7165
[11] J. P. Perdew, R. G. Parr, M. Levy, and J. L. Balduz, "Density functional theory for fractional particle number: derivative discontinuities of the energy,"*Physical Review Letters*, vol.49, no.23, pp. 1691–1694, 1982.https://doi.org/10.1103/PhysRevLett.49.1691
[12] C. G. Zhan, J. A. Nichols, and D. A. Dixon, "Ionization potential, electron affinity, electronegativity, hardness, and electron excitation energy: molecular properties from density functional theory orbital energies," *Journal of PhysicalChemistry A*, vol.107, no. 20, pp. 4184–4195, 2003. https://doi.org/10.1021/jp0225774
[13] G. Schwarzenbach, and H. Flaschka, (1999) *Complexometric Titrations*, 2nd Edn., Methuen and Co., London.http://dx.doi.org/10.1016/0003-2670(70)80085-x
[14] Irving H. M., and Rossetti H. S., *J. Chem. Soc*. (1954) 2904.; https://doi.org/10.1039/jr9540002904
[15] MadhumitaHazra, TanushreeDolar, AkhilPandey, Subrata Kumar Dev, and AnimeshPatra., Bioinorganic Chemistry and Applications vol. 2014 (2014), *Article ID* 104046. http://dx.doi.org/10.1155/2014/104046
[16] Atta-ur-Rehman, MI Choudhary and WJ Thomsen. *Bioassay techniques for drugs development;* Amsterdam, the Netherlands; (2001) Hardwood Academics. https://doi.org/10.3109/9780203304532
[17]] M.I. Hossain, A. Kumer, S.H. Begum, *Asian J. Phys. Chem. Sci.,* **2018**, *3*, 1-9. http://doi.org/10.9734/AJOPACS/2018/39148
[18] R. Parr and W. Yang, *Functional Heory of Atoms and Molecules*, Oxford University Press, New York, NY, USA,1989.

[19] G. Zhang and C. B. Musgrave, "Comparison of DFT methods for molecular orbital eigenvalue calculations," *Journal of Physical Chemistry A*, vol. 111, no. 8, pp. 1554–1561, 2007.
[20] Hanane Tabbi, Tahar Abbaz, Amel Bendjeddou, Didier Villemin, *Int. J. Pharm. Sci. Rev. Res.,* 47(2), 2017; Article No. 24, Pages: 133-141
[21] Pearson RG. Absolute electronegativity and hardness: applications to organic chemistry. J. Org. Chem. 54, 1989, 1423-1430. DOI: 10.1021/jo00267a034.
[22] Geerlings P, Proft FD, Langenaeker W. Conceptual density functional theory. Chem. Rev. 103, 2003, 1793-1873. DOI: 10.1021/cr990029p.
[23] Parr RG, Szentpály LV, Liu S. Electrophilicity index. J. Am. Chem. Soc. 121, 1999, 1922–1924. DOI: 10.1021/ja983494x.
[24] Scrocco E, Tomasi J. Electronic molecular structure, reactivity and intermolecular forces: An euristic interpretation by means of electrostatic molecular potentials. Adv. Quantum Chem. 11, 1978, 115-193. http://doi.org/10.1016/S0065-3276(08)60236-1
[25] Luque FJ, Lopez JM, Orozco M. Perspective on "Electrostatic interactions of a solute with a continuum. A direct utilization of ab initio molecular potentials for the prevision of solvent effects". Theor. Chem. Acc. 103, 2000, 343-345. http://doi.org/10.1007/s002149900013
[26] Chattaraj PK., Giri S. Stability, reactivity, and aromaticity of compounds of a multivalent superatom. J. Phys. Chem. A 111, 2007, 11116–11121. DOI: 10.1021/jp0760758.
[27] Padmanabhan J, Parthasarathi R, Subramaniaan V, Chattaraj PK. Electrophilicity-based charge transfer descriptor. J. Phys. Chem. A 111, 2007, 1358–1361.
[28] Shanthi, E., Nalini, C., Rama, A., The effect of highly-available epistemologies on hardware and architecture, International Journal of Pharmacy and Technology, V-8, I-3, PP-17082-17086, 2016.
[29] Sharavanan, R., Golden Renjith, R.J., Design and analysis of fuel flow in bend pipes, International Journal of Pure and Applied Mathematics, V-116, I-15 Special Issue, PP-59-64, 2017
[30] R. Nayan, and A. K. Dey, *Indian J. Chem*. 1972.10 : 109
[31] S. D. Russel, "*Physical Methods in Chemistry*", Saunders, Philadelphia (1977).ISBN 0-03-075176-4
[32] B. Gangadhar Bagihalli, P. S. Badami and S. A. Patil, *Journal of Enzyme inhibition and Medicinal Chemistry 2009*.http://dx.doi.org/10.1080/14756360802187901
[33]P.V.Anantha Lakshmi, P.Saritha Reddy, V. Jatayaga Raju, Synthesis, Characterization and antimicrobial activity of 3d transition metal complexes of a biambidentate ligand containing quinoxaline moiety, Spectrochim. Acta A 74 (2009), 52-57.
[34] P. Tharmaraj, D. Kodimunthiri, C.D. Sheela, C.S. Shanmuga Priya, Synthesis, spectral studies and antibacterial activity of Cu(II), Co(II), and Ni(II) complexes of 1-(2-hydroxy phenyl)-3- phenyl-2-propen-1-one, N2-[(3,5-dimethyl-1H-pyrazol-1-yl)methyl] hydrazone, J. Serb. Chem. Soc. 74 (2009) 927–938.
[35] N. Raman, Y. Pitchaikani Raja, A. Kulandaisawy, Synthesis and characterization of Cu (II), Ni (II), Mn (II), Zn (II) and Vo (II) Schiff base complexes derived from ophenylenediamine and acetoacetanilide, Proc. Indian Acad. Sci. (Chem. Sci.) 113,(2001) 183–189
[36] D. Kannan, M. N. Arumugham, *International Journal of Research in controlled Release*-2012.ISSN 2249-8540.,https://www..urpjournals.com.
[37] C. N. Sudhamani, H. S. BhojyaNaik, T. R. RavikumarNaik, M. C. Prabhakara, *Spectrochim. Acta*, Part A 72 (2009) 643.https://doi.org/ 10.1016/j.saa.2008.11.025.
[38] P. Krishnamoorthy, P.Sathyadevi, A. H. Cowley, R. R. Butorac, N. Dharmaraj; *Eur. Jour. Med. Chem*. 46 (2011) 3376-3387. https://doi.org/10.1016/j.ejmech.2011.05.001
[39] Joseyphus R. S., Nair M. S., *Arabian J Chem* (2010) 3, 195-204, http://dx.doi.org/10.1016/j.arabjc.2010.05.001